Published in final edited form as:
Mol Cancer Ther. 2009 June ; 8(6): 1589–1595. doi:10.1158/1535-7163.MCT-09-0038.

Vorinostat enhances the radiosensitivity of a breast cancer brain metastatic cell line grown *in vitro* and as intracranial xenografts

Andrew Baschnagel[1], **Andrea Russo**[1], **William E. Burgan**[2,4], **Donna Carter**[2,4], **Katie Beam**[2,3], **Diane Palmieri**[3], **Patricia S. Steeg**[3], **Philip Tofilon**[5], and **Kevin Camphausen**[1]

[1]Radiation Oncology Branch, National Cancer Institute, Bethesda, Maryland [2]Molecular Radiation Therapeutics Branch, National Cancer Institute, Bethesda, Maryland [3]Laboratory of Molecular Pharmacology, National Cancer Institute, Bethesda, Maryland [4]Science Applications International Corporation-Frederick, National Cancer Institute-Frederick, Frederick, Maryland [5]Drug Discovery Program, H. Lee Moffitt Cancer Center, Tampa, Florida

Abstract

Vorinostat (suberoylanilide hydroxamic acid), a histone deacetylase inhibitor, is currently undergoing clinical evaluation as therapy for cancer. We investigated the effects of vorinostat on tumor cell radiosensitivity in a breast cancer brain metastasis model using MDA-MB-231-BR cells. *In vitro* radiosensitivity was evaluated using clonogenic assay. Cell cycle distribution and apoptosis was measured using flow cytometry. DNA damage and repair was evaluated using γH2AX. Mitotic catastrophe was measured by immunostaining. Growth delay and intracranial xenograft models were used to evaluate the *in vivo* tumor radiosensitivity. Cells exposed to vorinostat for 16 hours before and maintained in the medium after irradiation had an increase in radiosensitivity with a dose enhancement factor of 1.57. γH2AX, as an indicator of double-strand breaks, had significantly more foci per cell in the vorinostat plus irradiation group. Mitotic catastrophe, measured at 72 hours, was significantly increased in cells receiving vorinostat plus irradiation. Irradiation of s.c. MDA-MB-231-BR tumors in mice treated with vorinostat resulted in an increase in radiation-induced tumor growth delay. Most importantly, animals with intracranial tumor implants lived the longest after combination treatment. These results indicate that vorinostat enhances tumor cell radiosensitivity *in vitro* and *in vivo*. There was a greater than additive improvement in survival in our intracranial model. Combining vorinostat with radiation may be a potential treatment option for patients with breast cancer who develop brain metastases.

Introduction

Histone acetylation, controlled by histone acetylases and histone deacetylases (HDAC), modifies nucleosome and chromatin structures and regulates gene expression (1). Although histone acetyltransferase inactivation has been associated with oncogenesis, it is the aberrant HDAC activity leading to transcriptional repression of tumor suppressor genes that is considered to be a common event contributing to tumor formation (2). Molecules that can inhibit HDACs and reverse the aberrant epigenetic changes associated with various cancers are currently being investigated as possible therapeutics.

Requests for reprints: Kevin Camphausen, Radiation Oncology Branch, National Cancer Institute, 10 Center Drive, Building 10, CRC, Room B2-3561, Bethesda, MD 20892. Phone: 301-496-4146;, Fax: 301-480-1434. camphauk@mail.nih.gov.

Disclosure of Potential Conflicts of Interest
No potential conflicts of interest were disclosed.

HDAC inhibitors have been shown to induce tumor cell differentiation, apoptosis, and/or growth arrest in several *in vitro* and *in vivo* experimental models. Multiple HDAC inhibitors have also been shown to affect radiosensitivity in preclinical models (3). One of these HDAC inhibitors, vorinostat (suberoylanilide hydroxamic acid), a novel synthetic hybrid polar compound, has been shown to inhibit HDAC activity and enhance radiosensitivity in multiple cell lines, including glioma (U373) and prostate (DU145) cell lines (4), a colorectal carcinoma cell line (HCT116; ref. 5), a pancreatic cell line (MiaPaca; ref. 6), two human melanoma cell lines (A375 and MeWo), and a non–small cell lung cancer cell line (A549; ref. 7). However, the combination of vorinostat and radiation *in vivo* has not been reported.

Thus, to build on and extend the current published data, we initially investigated *in vitro* whether vorinostat could radiosensitize three other commonly used cell lines: an ovarian cancer cell line (NCI/ADR-RES), a breast cancer cell line (T47D), and a breast cancer brain metastasis cell line (MDA-MB-231-BR). Because of the potential of combining vorinostat with radiotherapy in breast cancer patients with brain metastases, we focused on that cell line for the *in vivo* work.

The data presented indicate that vorinostat enhances the tumor radiosensitivity *in vitro* and *in vivo*. Moreover, the sensitization correlates with delayed dispersion of phosphorylated histone H2AX (γH2AX) and an increase in cells undergoing mitotic catastrophe. Most importantly, there was an increase in survival in animals with intracranial implants in the group receiving the combination treatments.

Materials and Methods

Cell Line and Treatment

The MDA-MB-231-BR, a breast tumor brain metastatic cell line (8, 9), was supplied by the laboratory of Patricia S. Steeg (National Cancer Institute, Bethesda, MD). NCI/ADR-RES cells, an ovarian adenocarcinoma cell line, and T47D cells, a breast adenocarcinoma cell line, were obtained from the American Type Culture Collection. Cells were grown in DMEM (Invitrogen) with glutamate (5 mmol/L) and 10% fetal bovine serum and maintained at 37°C, 5% CO_2. Vorinostat, generously provided by Merck & Co., was reconstituted in DMSO to a stock concentration of 75.5 mmol/L and stored at −20°C. Cultures were irradiated using a Pantak X-ray source at a dose rate of 2.28 Gy/min.

Histone Acetylation Analysis

The acetylation status of histone H3 was determined by immunoblot analysis as previously described (10). Briefly, after exposure to 1 μmol/L vorinostat and collection at designated time points, cells were scraped into PBS, washed, and resuspended in Masaki's lysis buffer. Proteins were solubilized by sonication and run on 4% to 12% SDS-PAGE gels (Invitrogen). Gels were transferred to polyvinylidene difluoride membranes (Invitrogen) and incubated overnight using antibodies to acetylated histone H3 (Upstate Biotechnology) or actin (Chemicon). Enhanced chemiluminescence Western blotting reagents (Santa Cruz Biotechnology) were used for development on a Fuji scanner (Kodak).

Clonogenic Assay

Cultures were trypsinized to generate a single-cell suspension and a specified number of cells were seeded into each well of a six-well tissue culture plate. After allowing cells time to attach (6 h), cultures received vorinostat (500 nmol/L or 1 μmol/L) or DMSO (vehicle control) for 16 h before irradiation and maintained in the medium after irradiation. Ten to 14 d after seeding, colonies were stained with crystal violet, the number of colonies containing at least 50 cells was determined, and surviving fractions were calculated. Survival curves

were then generated after normalizing for the amount of vorinostat-induced cell death. Data presented are the mean ± SE from at least three independent experiments.

Cell Cycle Analysis

Evaluation of cell cycle phase distribution was done using flow cytometry (Guava Technologies). Cells were seeded into 10-cm dishes, treated with 1 μmol/L vorinostat for 16 h, irradiated, and collected at designated times. For a positive control, cells were treated with 0.2 μg/mL nocodazole for 24 h before analysis. To evaluate the activation of the G_2 cell cycle checkpoint, mitotic cells were distinguished from G_2 cells and the mitotic index was determined according to the expression of phosphorylated histone H3 (Upstate Biotechnology). All observations were validated by at least three independent experiments.

Apoptotic Cell Death

The Guava Nexin assay (Guava Technologies) was done following the manufacturer's instructions. Cells were treated with 1 μmol/L vorinostat for 16 h, irradiated, and collected at designated times. Briefly, 2.0×10^4 to 1.0×10^5 cells (100 μL) were added to 100 μL of Guava Nexin Reagent. Cells were incubated in the dark at room temperature for 20 min and samples (2,000 cells per well) were then acquired on the Guava EasyCyte System. All observations were validated by at least three independent experiments.

Immunofluorescent Staining for γH2AX

Immunofluorescent staining and counting of γH2AX nuclear foci was done as previously described (10). Cells were treated with 1 μmol/L vorinostat for 16 h, irradiated, and fixed at designated times. Slides were examined on a Leica DMRXA fluorescent microscope. Images were captured by a Photometrics Sensys charge-coupled device camera (Roper Scientific) and imported into IP Labs image analysis software package (Scanalytics, Inc.). For each treatment condition, γH2AX foci were counted in at least 150 cells, with each count repeated three times.

Mitotic Catastrophe

The presence of fragmented nuclei was used as the criteria for defining cells undergoing mitotic cell death. Cells were treated with 1 μmol/L vorinostat for 16 h, irradiated, and fixed at designated times. To visualize nuclear fragmentation, cells were fixed with methanol for 15 min at −20°C and stained with mouse anti-tubulin antibody (Sigma-Aldrich) followed by staining with Texas red–conjugated secondary antibody (Jackson ImmunoResearch Laboratories, Inc.). Nuclei were counterstained with 4′,6-diamidino-2-phenylindole (Sigma). A single field containing 100 cells was selected at random for each treatment group and photographed with epifluorescence. Nuclear fragmentation was defined as the presence of two or more distinct nuclear lobes within a single cell. Cells undergoing cytokinesis were visually identified and excluded from the count. For each treatment condition, nuclei were counted in at least 100 cells with each count repeated three times.

In vivo Tumor Models

Four- to 6-wk-old female nude mice (Frederick Labs) were used in these studies. Mice were caged in groups of five or less, and all animals were fed a diet of animal chow and water *ad libitum*. Irradiation was done using a Pantak irradiator with animals restrained in a custom jig. All animal studies were conducted in accordance with the principles and procedures outlined in the NIH Guide for the Care and Use of Animals.

Tumor Growth Delay Assay

MDA-MB-231-BR tumor cells (5×10^6) suspended in saline were injected s.c. into the right hind leg. When tumors grew to a mean volume of 172 mm^3, mice were randomized into four groups: vehicle alone, vorinostat alone, irradiation alone, or vorinostat plus irradiation. The mice were given a single dose of vorinostat (50 mg/kg) by p.o. gavage 6 h before local tumor irradiation (3 Gy). To obtain tumor growth curves, perpendicular diameter measurements of each tumor were made every 2 d with digital calipers, and volumes were calculated using the following formula: $L \times W \times W/2$. Tumors were followed until the tumors of the group reached a mean size of >700 mm^3. Specific tumor growth delay was calculated for each individual animal in a treatment group as the number of days for the mean of the treated tumors to grow to 500 mm^3 minus the number of days for the mean of the control group to reach the same size. SEs in days were calculated from the mean of the treated groups. Each experimental group contained 5 mice; 10 mice were included in the control group.

Intracranial Xenograft Survival Model

Mice were anesthetized by i.p. injection of ketamine (83 mg/kg) and rompun (8.3 mg/kg) dissolved in saline. Using a blank syringe, 1×10^6 of MDA-MB-231-BR tumor cells suspended in 5 μL of PBS were injected into the caudate nucleus at a depth of 3 mm from the dura over 10 min. The needle was left in place for 2 min and then withdrawn slowly. The scalp wound was closed with 5-0 PDS suture. Surgery was done using sterile technique. Mice were placed on a heating pad in sterile cages and allowed to awaken from anesthesia. Three days after implantation, animals were randomized into one of four treatment groups: vehicle alone, vorinostat alone, irradiation alone, or vorinostat plus irradiation. The mice were given a single dose of vorinostat (75 mg/kg) by p.o. gavage 6 h before their single dose of radiation (5 Gy). Each experimental group contained five mice. The day of tumor implantation was assigned as day zero.

Statistical Analysis

In vitro experiments were repeated thrice and statistical analysis was done using a Student's *t* test. Data are presented as mean ± SE. A probability level of a *P* value of <0.05 was considered significant. Kaplan-Meier curves were used and a log-rank value was calculated for the intracranial survival implant model.

Results

The aim of this study was to investigate the effects of vorinostat on the radiosensitivity of a breast tumor brain metastasis model (MDA-MB-231-BR; refs. 8, 9). Previous studies have established a correlation between HDAC inhibitor–induced histone hyperacetylation and radiosensitization (10). Consistent with the transient nature of histone hyperacetylation, we have shown previously that maximum radiosensitization is obtained when cells are exposed to HDAC inhibitors both before and after irradiation (6, 10, 11). Consequently, we first defined vorinostat-induced hyperacetylation of MDA-MB-231-BR cells both immediately after drug exposure and after removal of drug. Cells were either exposed to vorinostat (1 μmol/L) for 16 hours and collected (time 0) or exposed to vorinostat (1 μmol/L) for 16 hours; medium was removed; and cells were rinsed with PBS, fed fresh drug-free medium, and collected after an additional 6 hours for immunoblot analysis. As shown in Fig. 1, vorinostat treatment leads to hyperacetylation of H3 that returns to baseline within 6 hours after drug removal. Based on these results, rather than remove vorinostat from the medium after irradiation as in previous studies (5), subsequent analyses of radiosensitization involved maintaining this HDAC inhibitor in the medium after irradiation.

To determine tumor cell radiosensitivity, clonogenic survival analysis was done. Three cell lines were used: MDA-MB-231-BR, NCI/ADR-RES, and T47D cells. MDA-MB-231-BR cells were exposed to varied concentrations of vorinostat for 16 hours before irradiation with drug maintained in the medium after irradiation. As shown in Fig. 2A, the dose enhancement factor (DEF) at a surviving fraction of 0.1 for MDA-MB-231-BR cells exposed to 500 nmol/L was 1.31 compared with a DEF of 1.57 in cells treated with 1 μmol/L vorinostat. The surviving fractions of MDA-MB-231-BR cells after continuous exposure were 0.89 ± 0.04 and 0.86 ± 0.06 for the 500 nmol/L and 1 μmol/L doses, respectively. To determine whether the vorinostat-induced radiosensitization was unique to the MDA breast cancer cells, studies were extended to two other cell lines. NCI/ADR-RES and T47D cells underwent the same continuous exposure protocol but were only exposed to 500 nmol/L vorinostat. A dose of 1 μmol/L was not used in these cell lines because 500 nmol/L vorinostat had a significant effect on the surviving fraction. The DEFs at a surviving fraction of 0.1, as shown in Fig. 2B/C, for NCI/ADR-RES and T47D were 1.50 and 1.21, respectively, with a surviving fraction to drug exposure only of 0.25 ± 0.08 and 0.41 ± 0.03, respectively. As suggested by previous studies, these results indicate that vorinostat is an effective *in vitro* radiosensitizing agent.

To address the mechanisms of vorinostat-induced radiosensitization *in vitro*, we focused on MDA-MB-231-BR cells treated with 1 μmol/L vorinostat for 16 hours with drug maintained in the medium after irradiation. The combination of vorinostat with irradiation has been reported to modify cell cycle distribution in some cell lines by increasing the number of cells in the G_2 phase (12). Because redistribution of cells in the cell cycle can affect radiosensitivity, flow cytometry was used to determine the cell cycle phase distribution of MDA-MB-231-BR cells exposed to1 μmol/L vorinostat for 16 hours and then collected 1, 6, and 24 hours after irradiation. Cells treated with vorinostat alone for 16 hours did not alter cell phase distribution (data not shown). There also was no difference in the cell cycle distribution for irradiated cells treated with or without the addition of vorinostat (data not shown). These results indicate that redistribution of cells into a radiosensitive phase of the cell cycle does not account for the vorinostat-mediated enhancement in radiation-induced cell killing observed in Fig. 2. It should be noted that the vorinostat concentration used to enhance radiosensitivity in this study was 1 μmol/L, whereas the concentration that affected the cell cycle distribution of an irradiated human melanoma cell line was 2.5 μmol/L (12).

Vorinostat has been reported to induce apoptosis in some tumor cell lines but not in others (4). To determine whether apoptosis is involved in the radiosensitization of MDA-MB-231-BR cells, Annexin staining was done in cells at 24, 48, and 72 hours following irradiation (2 Gy). As expected for a solid tumor cell line, radiation alone induced little apoptotic cell death and there was minimal increase in apoptosis after vorinostat/irradiation treatment, indicating that apoptosis is not the mechanism of vorinostat-mediated radiation-induced cell death (data not shown).

To measure radiation-induced DNA damage, we evaluated γH2AX expression. γH2AX foci expression has been established as a sensitive indicator of DNA double-strand breaks (DSB) and the dispersion of these foci has been shown to correspond to DSB repair in cells exposed to irradiation. Munshi et al. (7) have shown that vorinostat prolongs the expression of γH2AX in a melanoma cell line exposed to irradiation. As shown in Fig. 3, the combination of vorinostat plus irradiation had a statistically significant increase in the number of foci at 1, 6, 24, and 48 hours compared with cells treated with irradiation alone. Whereas at 48 hours the number of foci in cells receiving irradiation alone had returned to the nonradiated control level, foci in cells collected 48 hours after treatment with the combination of vorinostat and irradiation were still present, indicating an inhibition of DNA DSB repair. Interestingly, cells treated with vorinostat alone had an increase in the amount

of γH2AX above control levels that persisted when measured over time. This finding is new and has never been reported in the literature. When taking this finding into account, the number of γH2AX foci at 48 hours in cells treated with the combination of vorinostat and irradiation was still greater than additive when compared with cells treated with irradiation alone and vorinostat alone, indicating that the addition of vorinostat to irradiated cells enhances the inhibition of DNA DSB repair.

Because vorinostat inhibits DSB repair and does not cause a significant increase in radiation-induced apoptosis, we hypothesized that vorinostat-induced radiosensitization involves an enhancement of cells undergoing mitotic catastrophe. Mitotic cell death was determined according to the number of cells with abnormal nuclei (multinuclear giant cells or cells with several micronuclei) as a function of time after irradiation. As shown in Fig. 4, there was a time-dependent increase in the number of cells undergoing mitotic catastrophe after the treatment with irradiation alone and with vorinostat plus irradiation. In cells receiving the combination treatment, a significantly greater number of cells undergoing mitotic catastrophe were detected at 72 hours after treatment when compared with the irradiated alone cells. These results suggest that the vorinostat-induced radiosensitization is mediated by an inhibition of DSB repair, resulting in an increase in cells undergoing mitotic catastrophe.

To determine whether the enhancement of tumor cell radiosensitivity measured *in vitro* could be translated into an *in vivo* tumor model, a tumor growth delay assay using MDA-MB-231-BR cells grown s.c. in the hind leg of nude mice was used. Mice bearing s.c. xenografts (172 mm^3) were randomized into four groups: vehicle, vorinostat only (50 mg/kg), irradiation (3 Gy) only, and vorinostat (50 mg/kg) given 6 hours before irradiation (3 Gy). The average growth rates for the MDA-MB-231-BR tumors exposed to each treatment are shown in Fig. 5. For each group, the time to grow from 172 mm^3 (volume at the time of treatment) to 500 mm^3 was calculated using the tumor volumes from the individual mice in each group (mean ± SE). The time required for tumors to grow from 172 to 500 mm^3 increased from 6.7 ± 0.2 days for vehicle-treated mice to 8.6 ± 0.5 days for vorinostat-treated mice and 8.1 ± 0.9 days for irradiated-treated group. In mice that received the vorinostat plus irradiation combination, the time for tumors to grow to 500 mm^3 increased to 13.7 ± 0.7 days ($P < 0.01$ versus vehicle, irradiation, and vorinostat alone). The absolute growth delays (the time in days for tumors in treated mice to grow from 172 to 500 mm^3 minus the time in days for tumors to reach the same size in vehicle-treated mice) were 1.9 ± 0.3 for vorinostat alone and 1.4 ± 0.7 for irradiation alone, whereas the tumor growth delay induced by the vorinostat plus irradiation treatment was 7.0 ± 0.5 days. Thus, the growth delay after the combined treatment was more than the sum of the growth delays caused by individual treatments. To obtain a DEF comparing the tumor radioresponse in mice with and without vorinostat treatment, the normalized tumor growth delay was determined, which accounts for the contribution of vorinostat to tumor growth delay induced by the combination treatment. Normalized tumor growth delay is defined as the time in days for tumors to grow from 172 to 500 mm^3 in mice treated with the combination of vorinostat and radiation minus the time in days for tumors to grow from 172 to 500 mm^3 in mice treated with vorinostat only. The DEF, obtained by dividing the normalized tumor growth delay in mice treated with the vorinostat/radiation combination by the absolute growth delay in mice treated with radiation only, was 3.6. These results indicate that vorinostat significantly enhances the radiation-induced tumor growth delay of MDA-MB-231-BR xenografts.

To further evaluate the clinical potential of the vorinostat plus radiation combination, we extended the *in vivo* observations to an intracranial implant xenograft survival model. After undergoing intracranial implantation, groups of five mice were randomized into control, irradiation (5 Gy), vorinostat (75 mg/kg), or vorinostat (75 mg/kg) plus irradiation (5 Gy)

groups. The median survival in the control group was 13 days, whereas the median survival in the irradiation group and the vorinostat group was 16 days each. However, in the mice treated with the combination of vorinostat and irradiation, the median survival was 27 days ($P = 0.038$, by log-rank test). Thus, as shown in Fig. 6, there was a greater than additive effect on survival using the combination of vorinostat and irradiation when compared with each individual treatment in this clinically relevant model of breast cancer brain metastasis.

Discussion

Brain metastases are the most common intracranial tumor occurring in approximately 10% to 30% of adult cancer patients and are a major cause of morbidity and mortality (13). The risk of developing brain metastases varies according to primary tumor type, with breast cancer accounting for approximately 20% to 30% of all brain metastasis patients. The prognosis for these patients is poor, and without therapeutic intervention, the median survival time is 1 month (14). Whole brain radiation therapy, the standard of care for the majority of these patients, can relieve symptoms and results in a median survival of 4 to 6 months (15). As there are limited options available for these patients, agents that can optimize the therapeutic ratio and enhance the benefits of whole brain radiation therapy are currently being investigated.

HDAC inhibitors are a class of therapeutics that have great promise as radiosensitizing agents. Vorinostat is undergoing combination phase II clinical trials with various chemotherapies and a phase III trial in patients with malignant mesothelioma and has been Food and Drug Administration approved for patients with cutaneous T-cell lymphoma who have failed prior therapies (16). Vorinostat is orally administered and has been shown to readily cross the blood-brain barrier (17). Data from clinical trials show that it is well tolerated and has limited toxicities that are rapidly reversible on discontinuation of the drug (16, 18, 19). All of these characteristics as well as the wealth of preclinical data make vorinostat appealing as a radioenhancer of whole brain radiation therapy.

Thus, the goal of this study was to investigate the effects of vorinostat in a breast cancer brain metastasis model. Using the breast cancer brain metastasis cell line MDAMB- 231-BR, we have shown vorinostat-induced radiosensitization both *in vitro* and *in vivo* for s.c. and intracranial xenografts. Although the specific mechanism of HDAC enhancement of radiosensitivity remains unclear, it seems to be related to the pathways involved in the repair of DNA damage (4, 7, 10, 12, 20). An important determinant of radiosensitivity is the repair of radiation-induced DNA DSBs. Vorinostat has been shown to reduce the expression of the DNA repair–related proteins Ku70, Ku80, DNA-PK, Rad50, and Rad51 and prolong the expression of γH2AX, an indicator of DNA DSBs (4, 7). Our *in vitro* results support the idea that a major cause of vorinostat radiation-induced cell death involves inhibition of DSB repair, leading to mitotic cell death.

To our knowledge and at the time of this publication, this is one of the first reports of a vorinostat enhancing radiation response *in vivo*. In our s.c. xenograft model, vorinostat plus irradiation had a greater than additive effect on tumor growth delay. More importantly, mice implanted with MDA-MB-231-BR cells using our intracranial implant model treated with the vorinostat/irradiation combination showed an increase in median survival compared with mice treated with either irradiation or vorinostat alone. In both tumor models, vorinostat was well tolerated with minimal signs of toxicity. There were no premature deaths and mice in all groups maintained similar weights throughout the study.

Thus, our results support the possibility of a therapeutic benefit of combining vorinostat with radiation and warrant the investigation of this combination in clinical trials. Patients

with brain metastases should be the ideal patient population for the study of the radiosensitizing effects of vorinostat as their high local failure rate makes any improvement in local control and thus progression-free survival of significant benefit.

Acknowledgments

Grant support: Intramural Research Program of the NIH, National Cancer Institute, Center for Cancer Research and Department of Defense Breast Cancer Research Program grant W81 XWH-062-0033 (P.S. Steeg and K. Camphausen). A. Baschnagel was supported through the Clinical Research Training Program, a public-private partnership supported jointly by the NIH and Pfizer, Inc. (via a grant to the Foundation for NIH from Pfizer, Inc.).

References

1. Thiagalingam S, Cheng KH, Lee HJ, Mineva N, Thiagalingam A, Ponte JF. Histone deacetylases: unique players in shaping the epigenetic histone code. Ann N Y Acad Sci. 2003; 983:84–100. [PubMed: 12724214]
2. Johnstone RW. Histone-deacetylase inhibitors: novel drugs for the treatment of cancer. Nat Rev Drug Discov. 2002; 1:287–299. [PubMed: 12120280]
3. Camphausen K, Tofilon PJ. Inhibition of histone deacetylation: a strategy for tumor radiosensitization. J Clin Oncol. 2007; 25:4051–4056. [PubMed: 17827453]
4. Chinnaiyan P, Vallabhaneni G, Armstrong E, Huang SM, Harari PM. Modulation of radiation response by histone deacetylase inhibition. Int J Radiat Oncol Biol Phys. 2005; 62:223–229. [PubMed: 15850925]
5. Flatmark K, Nome RV, Folkvord S, et al. Radiosensitization of colorectal carcinoma cell lines by histone deacetylase inhibition. Radiat Oncol. 2006; 1:25. [PubMed: 16887021]
6. Cerna D, Camphausen K, Tofilon PJ. Histone deacetylation as a target for radiosensitization. Curr Top Dev Biol. 2006; 73:173–204. [PubMed: 16782459]
7. Munshi A, Tanaka T, Hobbs ML, Tucker SL, Richon VM, Meyn RE. Vorinostat, a histone deacetylase inhibitor, enhances the response of human tumor cells to ionizing radiation through prolongation of γ-H2AX foci. Mol Cancer Ther. 2006; 5:1967–1974. [PubMed: 16928817]
8. Yoneda T, Williams PJ, Hiraga T, Niewolna M, Nishimura R. A bone-seeking clone exhibits different biological properties from the MDA-MB-231 parental human breast cancer cells and a brain-seeking clone *in vivo* and *in vitro*. J Bone Miner Res. 2001; 16:1486–1495. [PubMed: 11499871]
9. Palmieri D, Bronder JL, Herring JM, et al. Her-2 overexpression increases the metastatic outgrowth of breast cancer cells in the brain. Cancer Res. 2007; 67:4190–4198. [PubMed: 17483330]
10. Camphausen K, Burgan W, Cerra M, et al. Enhanced radiation-induced cell killing and prolongation of γH2AX foci expression by the histone deacetylase inhibitor MS-275. Cancer Res. 2004; 64:316–321. [PubMed: 14729640]
11. Camphausen K, Scott T, Sproull M, Tofilon PJ. Enhancement of xenograft tumor radiosensitivity by the histone deacetylase inhibitor MS-275 and correlation with histone hyperacetylation. Clin Cancer Res. 2004; 10:6066–6071. [PubMed: 15447991]
12. Munshi A, Kurland JF, Nishikawa T, et al. Histone deacetylase inhibitors radiosensitize human melanoma cells by suppressing DNA repair activity. Clin Cancer Res. 2005; 11:4912–4922. [PubMed: 16000590]
13. Johnson JD, Young B. Demographics of brain metastasis. Neurosurg Clin N Am. 1996; 7:337–344. [PubMed: 8823767]
14. Zimm S, Wampler GL, Stablein D, Hazra T, Young HF. Intracerebral metastases in solid-tumor patients: natural history and results of treatment. Cancer. 1981; 48:384–394. [PubMed: 7237407]
15. Borgelt B, Gelber R, Kramer S, et al. The palliation of brain metastases: final results of the first two studies by the Radiation Therapy Oncology Group. Int J Radiat Oncol Biol Phys. 1980; 6:1–9. [PubMed: 6154024]

16. Mann BS, Johnson JR, He K, et al. Vorinostat for treatment of cutaneous manifestations of advanced primary cutaneous T-cell lymphoma. Clin Cancer Res. 2007; 13:2318–2322. [PubMed: 17438089]

17. Hockly E, Richon VM, Woodman B, et al. Suberoylanilide hydroxamic acid, a histone deacetylase inhibitor, ameliorates motor deficits in a mouse model of Huntington's disease. Proc Natl Acad Sci U S A. 2003; 100:2041–2046. [PubMed: 12576549]

18. Kelly WK, O'Connor OA, Krug LM, et al. Phase I study of an oral histone deacetylase inhibitor, suberoylanilide hydroxamic acid, in patients with advanced cancer. J Clin Oncol. 2005; 23:3923–3931. [PubMed: 15897550]

19. Luu TH, Morgan RJ, Leong L, et al. A phase II trial of vorinostat (suberoylanilide hydroxamic acid) in metastatic breast cancer: a California Cancer Consortium Study. Clin Cancer Res. 2008; 14:7138–7142. [PubMed: 18981013]

20. Camphausen K, Cerna D, Scott T, et al. Enhancement of *in vitro* and *in vivo* tumor cell radiosensitivity by valproic acid. Int J Cancer. 2005; 114:380–386. [PubMed: 15578701]

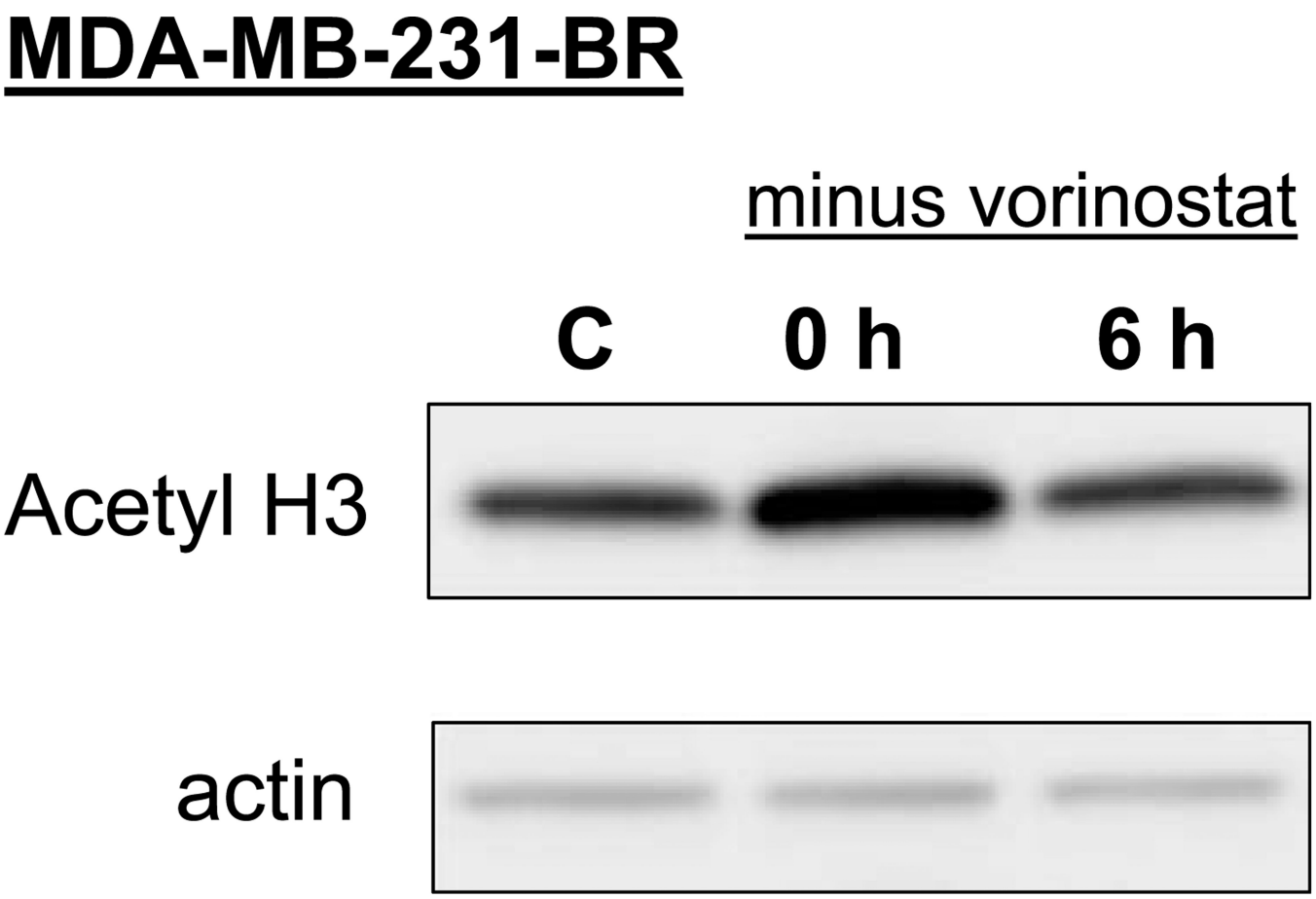

Figure 1.
Histone acetylation status determined after exposure to and removal of vorinostat. MDA-MB-231-BR cells were either exposed to vorinostat (1 μmol/L) for 16 h and collected (time 0 h) for immunoblot analysis of acetylated histone H3 or exposed to vorinostat (1 μmol/L) for 16 h; medium was removed; and cells were rinsed with PBS, fed fresh drug-free medium, and collected 6 h later for immunoblot analysis. *C,* cultures exposed to the vehicle only (DMSO).

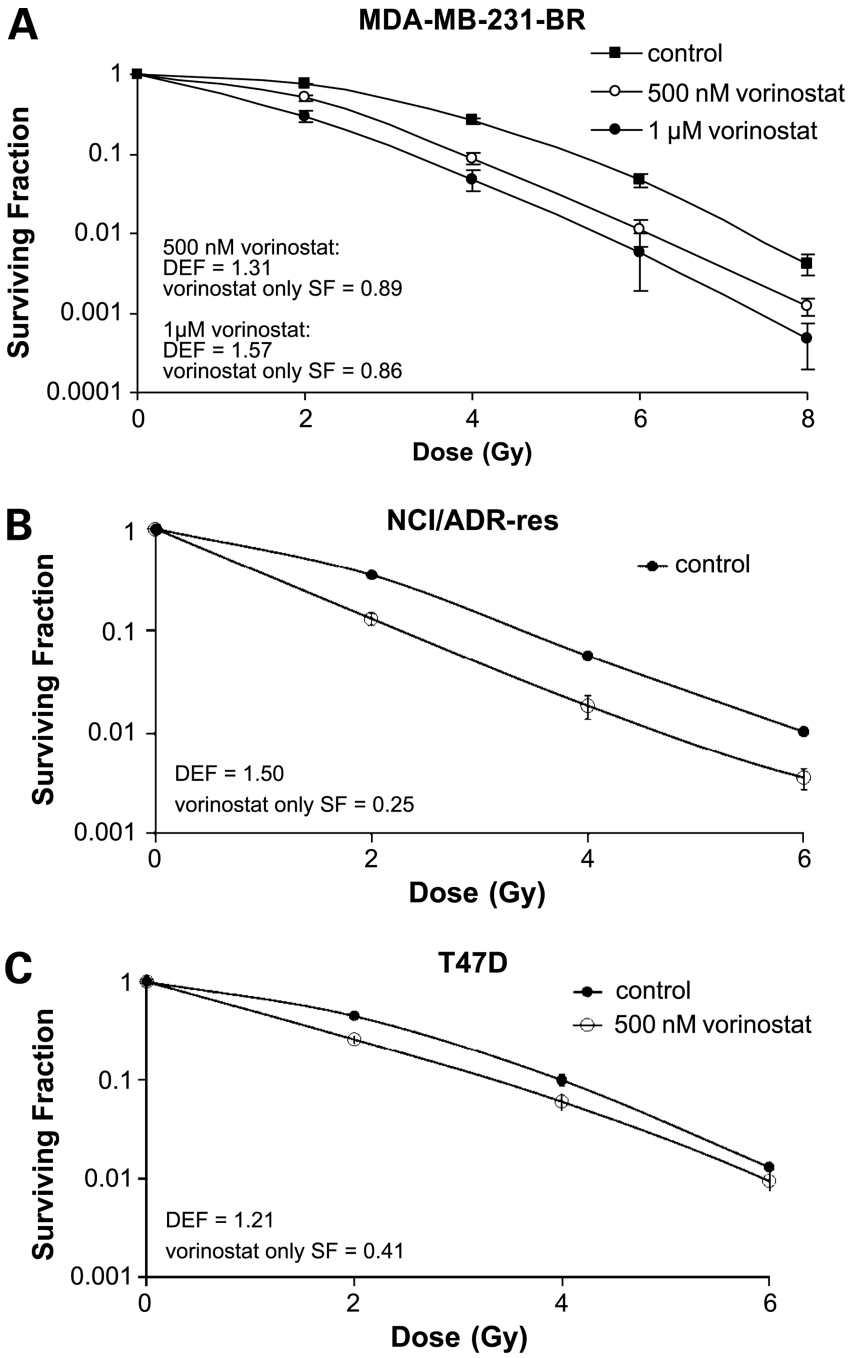

Figure 2.

The radiosensitivity effects of vorinostat on (**A**) MDA-MB-231-BR, (**B**) NCI/ADR-RES, and (**C**) T47D cells. Cell cultures were exposed to 500 nmol/L or 1 μmol/L of vorinostat for 16 h before irradiation and maintained in the medium after irradiation. Colony-forming efficiency was determined 10 to14 d later and survival curves were generated after normalizing for the cytotoxicity induced by vorinostat alone. *Points,* mean; *bars,* SE. *SF,* surviving fraction.

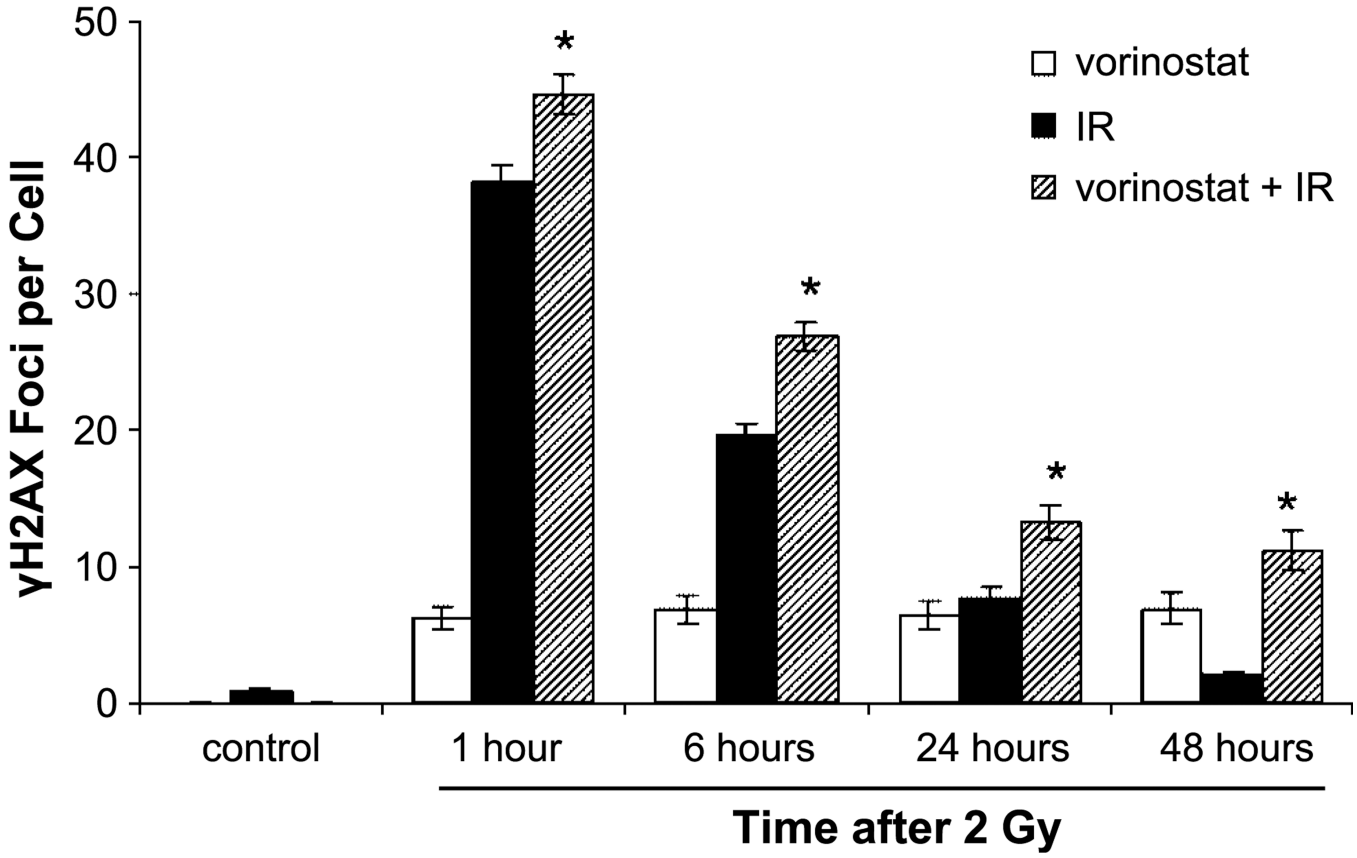

Figure 3.

γH2AX foci results of MDA-MB-231-BR cells. *White columns,* cells treated with vorinostat (1 μmol/L) alone; *black columns,* cells treated with irradiation (*IR*; 2 Gy) alone; *hatched columns,* cells treated with the combination of vorinostat (1 μmol/L) and irradiation (2 Gy). Control (*first black column*) refers to cultures exposed to vehicle (DMSO) following the same protocol. Vorinostat was given 16 h before treatment and maintained in the medium until cells were collected at designated time points. *Columns,* mean; *bars,* SE. *, $P < 0.01$, according to Student's *t* test (irradiation versus vorinostat plus irradiation).

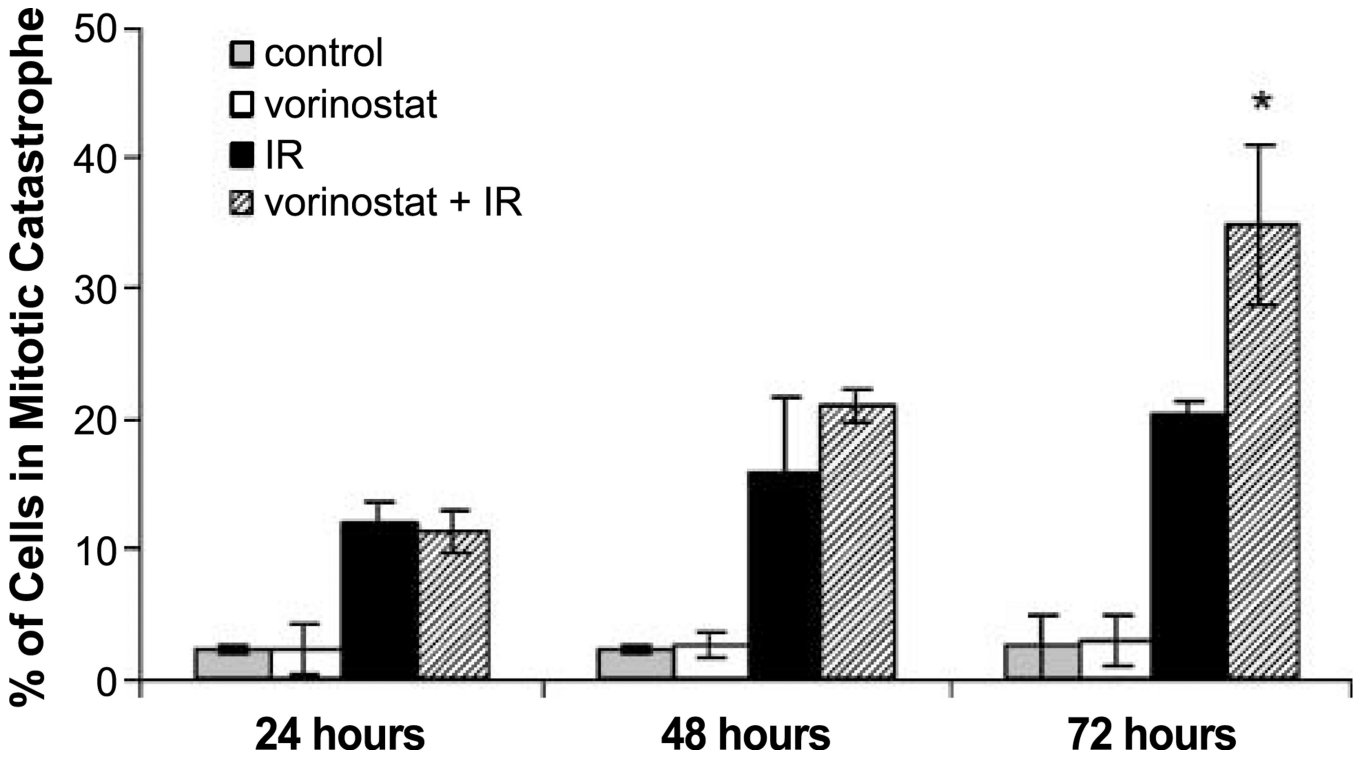

Figure 4.

Mitotic catastrophe results of MDA-MB-231-BR cells. *Gray columns,* vehicle-treated cells; *white columns,* cells treated with vorinostat (1 μmol/L) alone; *black columns,* cells treated with irradiation alone (2 Gy); *hatched columns,* cells treated with the combination of vorinostat (1 μmol/L) and irradiation (2 Gy). Vorinostat was given 16 h before treatment and maintained in the medium until cells were collected at designated time points. *Columns,* mean; *bars,* SE. Nuclear fragmentation was defined as the presence of two or more distinct lobes within a single cell. *, $P < 0.01$, according to Student's *t* test (irradiation versus vorinostat + irradiation).

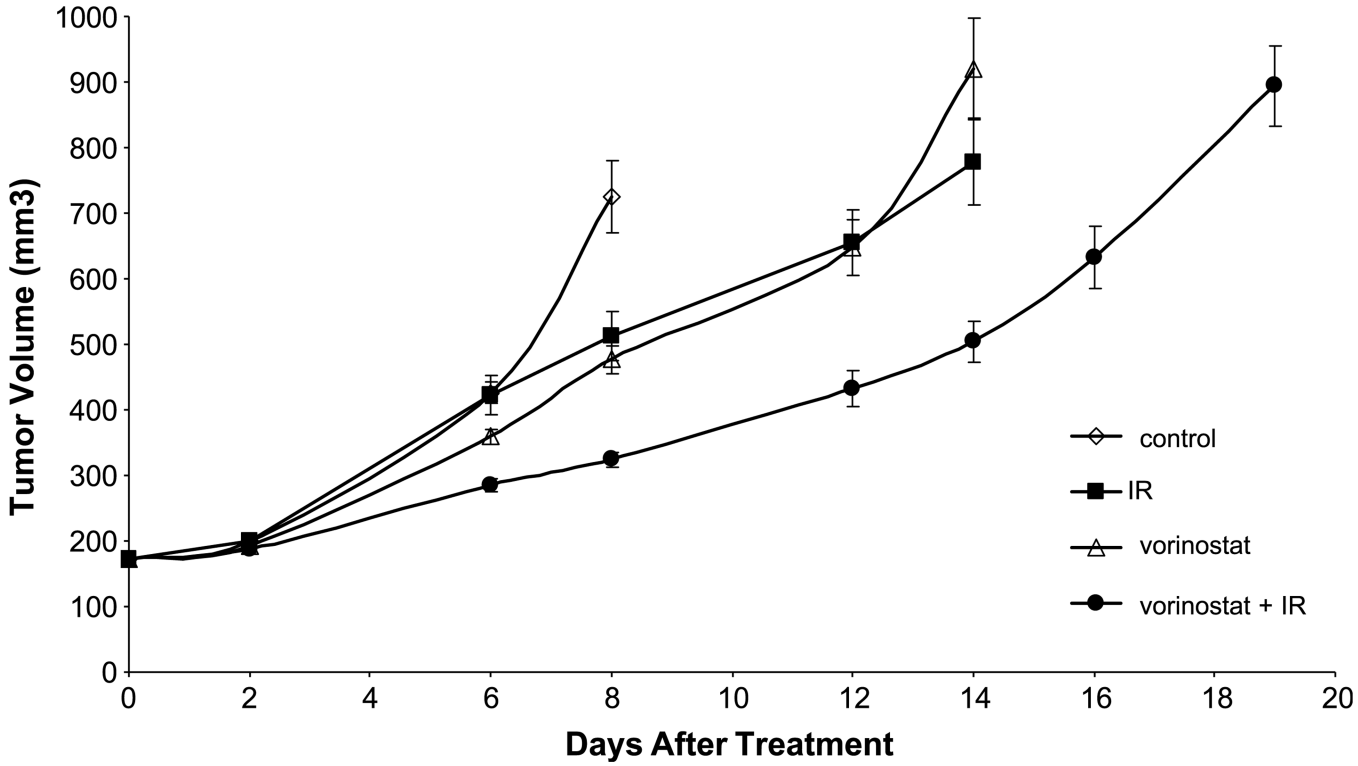

Figure 5.

The effects of vorinostat on radiation-induced MDA-MB-231-BR tumor growth delay. *Points,* mean tumor volume in mice after treatment with vorinostat, irradiation, or vorinostat ± irradiation; *bars,* SD. When tumors reached 172 mm^3 in size, mice were randomized into four groups: vehicle, vorinostat (50 mg/kg), irradiation (3 Gy), or vorinostat plus irradiation (50 mg/kg, 3 Gy). A single dose of vorinostat was delivered as p.o. gavage at 6 h before 3 Gy to the tumor. To obtain a tumor growth curve, perpendicular diameter measurements of each tumor were measured every 2 d with digital calipers, and volumes were calculated using the following formula: $L \times W \times W/2$. Each group contained five mice except control group, which contained 10 mice.

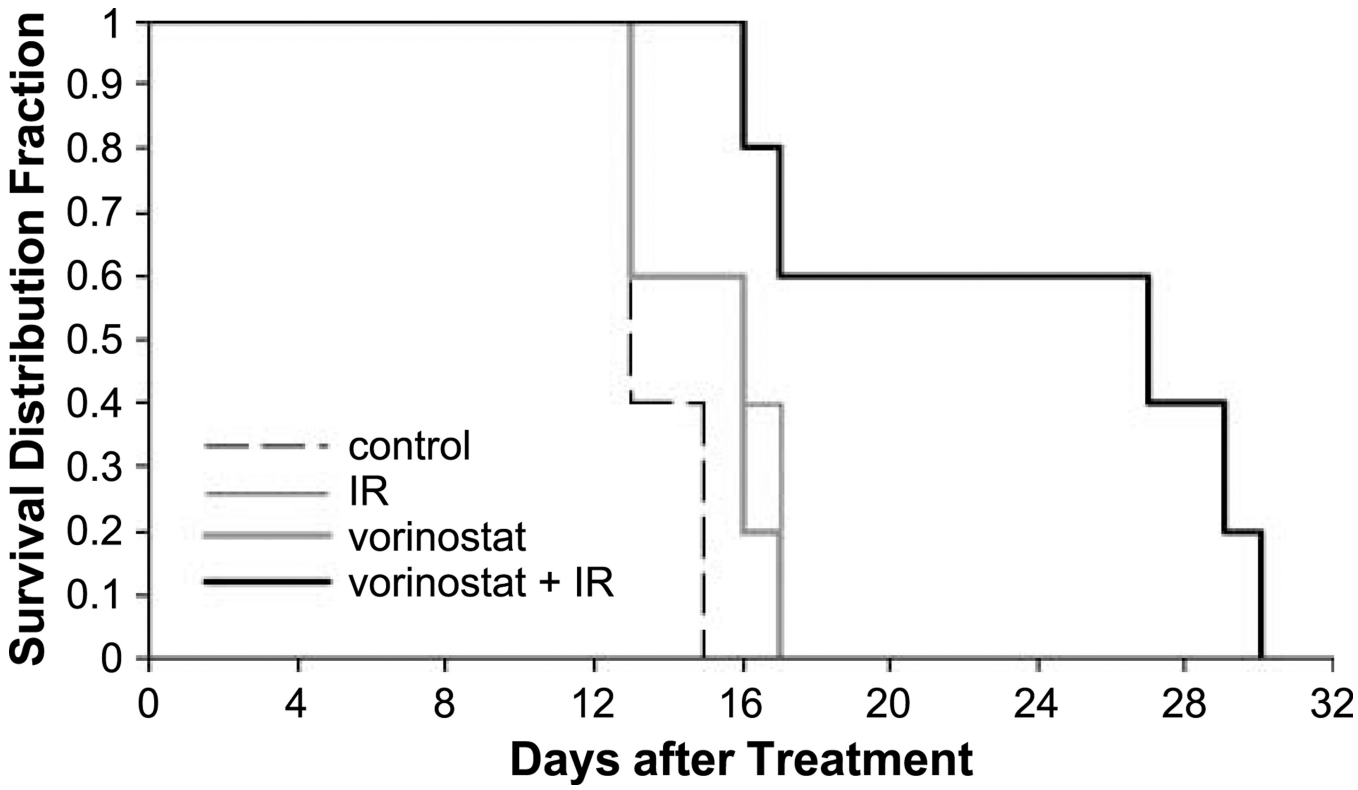

Figure 6.

Kaplan-Meier curve showing survival of mice with implanted intracranial MDA-MB-231-BR tumors and randomized to either control, irradiation (5 Gy), vorinostat (75 mg/kg), or vorinostat (75 mg/kg) plus irradiation (5 Gy). A single dose of vorinostat was delivered as p.o. gavage at 6 h before receiving 5 Gy. Each group contained five mice. $P = 0.038$, log-rank test (5 Gy versus vorinostat plus 5 Gy).